CrossMark

Thermal hazard evaluation of cyclohexanone peroxide synthesis

Na Zang[1,2] · Xin-Ming Qian[3] · Zhen-Yi Liu[3] · Chi-Min Shu[4]

Abstract Cyclohexanone peroxide, a crucial organic peroxide used as a curing agent or an initiator in free radical polymerization, is produced through a reaction of cyclohexanone with hydrogen peroxide in the presence of nitric acid as the catalyst. For this study, we used reaction calorimeter, differential scanning calorimetry, and accelerating rate calorimeter to evaluate the thermal hazard characteristics of cyclohexanone peroxide synthesis and the thermal stability of cyclohexanone peroxide. The overall kinetic parameters of the peroxide reaction, which were calculated based on the Levenberg–Marquardt algorithm, were validated using experimental data. By combining the maximum temperature of the synthesis reaction that was corrected by the yield and temperature, at which time to the maximum rate under adiabatic decomposition conditions was equal to 24 h, criticality classes were depicted to assess the cooling failure scenario of the peroxide reaction. This study enhances our understanding of the peroxide reaction and presents safer operating conditions and design protection measures for a safer and greener chemical industry.

✉ Na Zang
  zangnaduoduo@163.com

1   Department of Fire Protection Engineering, Chinese People's Armed Police Force Academy, Langfang 065000, Hebei, People's Republic of China

2   Jiangsu Key Laboratory of Urban and Industrial Safety, Nanjing University of Technology, Nanjing 211800, Jiangsu, People's Republic of China

3   State Key Laboratory of Explosion Science and Technology, Beijing Institute of Technology, Beijing 100081, People's Republic of China

4   Center for Process Safety and Industrial Disaster Prevention, School of Engineering, National Yunlin University of Science and Technology, Douliou, Yunlin 64002, Taiwan, ROC

List of symbols

A	Frequency factor (mol^{1-n} L^{n-1} s^{-1})
C_p	Specific heat capacity (kJ kg^{-1} K^{-1})
C_{p1}	Specific heat capacity of the reactant before the $RC1^e$ test (kJ kg^{-1} K^{-1})
C_{p2}	Specific heat capacity of the product after the $RC1^e$ test (kJ kg^{-1} K^{-1})
E_a	Apparent activation energy (kJ mol^{-1})
m_{cy}	Mass of cyclohexanone that has been dosed into the reaction (kg)
M_{cy}	Overall mass of cyclohexanone dosed into the reactor (kg)
M_r	Reactant mass in the reactor (kg)
m_T	Self-heating rate at an arbitrary temperature (°C min^{-1})
$MTSR$	Maximum temperature of the synthesis reaction (°C)
MTT	Maximum temperature for technical reasons (°C)
Q_{accu}	Accumulated energy (kJ)
Q_{exo}	Measured heat generation (kJ)
Q_{input}	Potential input energy (kJ)
Q_r	Heat release rate (W)
R	Gas constant 8.314 (J mol^{-1} K^{-1})
T	Temperature (°C)
T_{cf}	Maximum adiabatic temperature rise at a given time due to thermal accumulation (°C)
T_{D24}	Temperature at which TMR_{ad} is equal to 24 h (°C)

T_f	Measured final temperature during the ARC experiment (°C)
TMR_{ad}	Time to maximum rate under adiabatic decomposition conditions (min)
T_{onset}	Exothermic onset temperature (°C)
T_p	Reaction temperature (°C)
Y	Yield of the peroxide reaction (dimensionless)
β	Heating rate (°C min^{-1})
ΔH	Overall heat of reaction (kJ kg^{-1})
ΔT	Temperature rise (°C)
ΔT_{ad}	Adiabatic temperature rise (°C)

Superscript

a   Parameters from experimental data without correction
b   Parameters corrected by the yield

Introduction

Chemical industries have inherent thermal risks because of numerous hazardous materials and complex equipment. Many nations focus on high-energy chemicals, such as organic peroxides (OPs), and on using various methods and instruments for identifying reaction characteristics to prevent an operating system from potential thermal runaway hazards. OPs are commonly used as curing agents or initiators for polymerization because they easily yield free radicals. Several hazardous fires and explosions have occurred because of the unstable thermal decomposition properties of OPs; therefore, many studies have examined the hazard characteristics of OPs [1–10]. OPs have a sensitive chemical structure and an O–O bond that can readily decompose, releasing large amounts of heat under various unexpected conditions, such as overpressure, high temperature, incompatible substances, mechanical shock, or even ultraviolet radiation. Therefore, the use or production of OPs is of a major concern and warrants caution.

Cyclohexanone peroxide (CYHPO), a typical OP, is frequently used as a curing agent for sheet-molding compound and bulk-molding compound processes. CYHPO is synthesized through an acid (HNO₃)-catalyzed reaction of cyclohexanone with hydrogen peroxide (H₂O₂). Th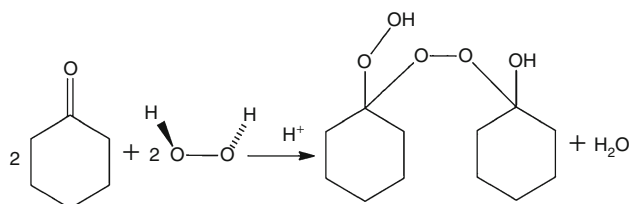e scheme for this reaction is shown in Fig. 1. However, this reaction is violently exothermic. On June 19, 2012, in Beijing, China, a severe explosion occurred involving the use of CYHPO [5]. Basic scientific safety data on the production of CYHPO are lacking. Various operating conditions, such as over-temperature and pressure, cooling failure, feed error, or incorrect dosing, may trigger a runaway reaction or even result in a fire, explosion, or toxic release [11–15]. In addition, according to the State Administration of Work Safety of China, during the 2009–2013 period, 1 of 18 dangerous chemical processes involved peroxide oxidation [16, 17]. Therefore, the related exothermic and thermokinetic features of CYHPO should be established to identify a suitable control mechanism for studying the thermal hazard characteristics of CYHPO.

We employed calorimetric methods to evaluate the inherent thermal hazard characteristics of CYHPO synthesis. First, a reaction calorimeter (RC1^e) was used to investigate the thermal behavior of CYHPO by scaling down the industrial conditions. The kinetic parameters were subsequently calculated through nonlinear optimization based on the Levenberg–Marquardt algorithm with the data obtained from RC1^e. To validate the kinetic model, this simulation was compared with that obtained from another RC1^e experiment. Differential scanning calorimetry (DSC) was used to test CYHPO to screen the influence of acids and impurities on secondary decomposition. In addition, an accelerating rate calorimeter (ARC) was used to investigate the thermal stability of CYHPO under adiabatic conditions. The cooling failure scenario was systematically evaluated to determine the hazard classification of the peroxide reaction. As a proactive measure, these procedures may be used for optimizing the operating conditions of the peroxide chemical reaction to prevent catastrophic industrial accidents.

Experimental

Samples

Analytical-grade cyclohexanone (≥99.5 mass%), H₂O₂ (≥30.0 mass%), and nitric acid (HNO₃) (65.0–68.0 % purity) were purchased from Aladdin Chemistry, Ltd., Shanghai, China.

Reaction calorimeter

A reaction calorimeter (RC1^e; METTLER-TOLEDO) was used for reaction safety analysis. The thermal behavior of CYHPO synthesis was investigated using RC1^e, which was equipped with an MP10 reactor. During RC1^e experiments, 58.0 g of H₂O₂ and 2.0 g of HNO₃ were introduced into the reactor. This mixture was then cooled to a temperature at

Fig. 1 Reaction scheme of the CYHPO synthesis

250 RPM. Next, 166.0 g of cyclohexanone was added to the reactor in isothermal mode. Operating parameters such as the heat generation rate, temperature, and dosing rate were recorded automatically. After RC1[e] experiments, the CYHPO yield was calculated based on product purification.

Differential scanning calorimetry

To assess real chemical industry conditions, a sample (sample 1) used in the DSC experiments was obtained at the end of the main reaction, which was the product obtained after the RC1[e] experiments. Temperature-programmed screening experiments were conducted using a METTLER-TOLEDO system equipped with a DSC1-measuring cell that could withstand pressure of up to 15.0 MPa. The calorimeter was calibrated using the manufacturer-supplied sapphire disk and indium standard by following the instrument calibration guidelines. For superior thermal equilibration, the heating rates (β) were selected to be 1.0, 2.0, 4.0, 8.0, and 10.0 °C min^{-1}. The range of temperature rise was 30.0–300.0 °C, and that of the sample mass was 2.0–5.0 mg in closed gold-plated crucibles. The reference was a pure gold-plated cell. The tests were conducted under ambient pressure and in a dry nitrogen atmosphere at a flow rate of 30.0 mL min^{-1}.

Accelerating rate calorimeter

An ARC (Thermal Hazard Technology, UK) can be used to effectively evaluate the thermal hazards of reactive substances under adiabatic conditions [18]. The standard ARC program of heat-wait-search was deliberately chosen, and experiments were performed with ambient pressure. For each ARC experiment, approximately 0.5 g of sample 1 was loaded in a lightweight spherical titanium alloy bomb (diameter, 2.5 cm). The initial temperature was set to 40.0 °C, and the final (end) temperature was set to 250.0 °C. The system temperature was raised by intervals of 5.0 °C at a heating rate of 0.02 °C min^{-1}. The waiting time was 10.0 min. After the self-heating rate exceeded the selected threshold of 0.02 °C min^{-1}, an exothermic reaction was recorded in the system. The pressure range was from the ambient pressure to 20.0 MPa.

Results and discussion

Thermal behavior of the isothermal peroxide reaction in RC1[e] experiments

Based on real chemical industry conditions, a conservative approach was to maintain the temperature below 20.0 °C during CYHPO synthesis. Therefore, our initial RC1[e] experiments were performed at 12.0, 15.0, and 18.0 °C. The heat generation rate and corresponding dosing curves are shown in Fig. 1.

As shown in Fig. 1, the Q_r curve at 15.0 °C exhibits an increasing trend with the constant feeding rate until the curve reaches a maximum value. The peroxide reaction rate decreases with the reactant concentration until the end of the dosing step. When the dosing time was approximately 150.0 min, a sharp spike was observed in the reaction heat (Fig. 2). To confirm this phenomenon, which was caused by a physical factor or secondary reaction, another RC1[e] experiment was conducted with the same reaction temperature, stirring rate, and dosing rate by scaling down the reactant concentration. As shown by the exothermic curve in Fig. 3, the sharp spike was not observed. Furthermore, the white solid crystal was reduced in the reactor. Therefore, the sharp spike was believed to have occurred because of positive thermal crystallization. During crystallization, liquids change to solids, molecular arrangement tends toward that of a regular crystal, internal energy decreases, and heat is
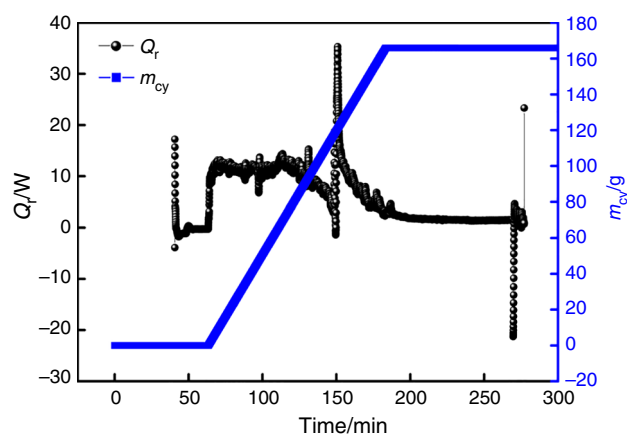

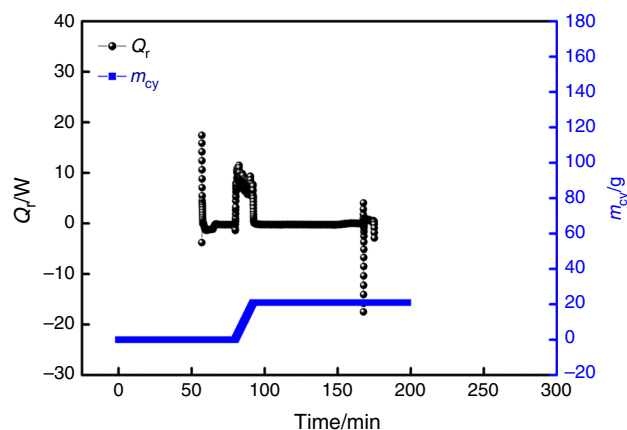**Fig. 2** Typical exothermic curves of the CYHPO synthesis at 15.0 °C

Fig. 3 Heat jump verification experiment of the CYHPO synthesis

Table 1 Thermal behavior parameters of RC1^e tests under various reaction conditions

Test no.	Reaction temperature/°C	Stirring rate/rpm	M_{cy}/g	Dosing time/min	$C_{p1} \times 10^{-1}$/ kJkg^{-1} K^{-1}	$C_{p2} \times 10^{-1}$/ kJ kg^{-1} K^{-1}	$\Delta H \times 10^{-1}$/kJ	Y/%
1	12.0	250	166.0	120.0	38.3	26.9	655.6	94.2
2	15.0	250	166.0	120.0	38.6	27.4	671.5	95.4
3	18.0	250	166.0	120.0	39.2	28.5	751.6	96.2
4	12.0	200	166.0	120.0	40.2	27.5	645.2	93.8
5	12.0	250	166.0	115.0	38.4	26.7	723.6	94.6
6	12.0	300	166.0	120.0	39.8	27.6	730.9	94.2
7	12.0	250	150.0	113.0	38.6	26.6	627.6	94.6
8	12.0	250	166.0	125.0	38.5	28.5	640.8	94.3
9	12.0	250	210.0	158.0	38.8	26.9	875.2	92.7

C_{p1}, heat capacity of the reactant before the RC1^e test; C_{p2}, specific heat capacity of the product after the RC1^e test; $\Delta T_{ad,r}$, adiabatic temperature increase in the desired reaction

released to form a lattice. Accordingly, a sharp rise in heat is observed.

The thermal behavior parameters of CYHPO synthesis are listed in Table 1. The specific heat capacity of the reactants ranged from 3.83 to 4.02 kJ kg^{-1} K^{-1}, and that of the peroxide product mixed with acid ranged from 2.66 to 2.85 kJ kg^{-1} K^{-1}. In addition, based on various reaction conditions, the internal substances of products and side reactions were different. The overall reaction heat of CYHPO synthesis ranged from 62.8 to 87.5 kJ.

Compared with Tests 1, 4, and 6, the overall reaction heat and adiabatic temperature rise of the desired reaction increased with the stirring rate. The stirring rate, which suggested changes in the liquid–liquid interfacial area, obviously reflected the reaction rate of heterogeneous liquid–liquid semi-batch reactors. CYHPO synthesis mainly involves an interfacial reaction; the high stirring rate accelerated both the reaction and heat transfer rates. Therefore, when the stirring rate was switched off suddenly and turned on again, an adiabatic temperature rise was observed at approximately 50 °C for Test 9, which may have caused a secondary reaction or thermal runaway scenario. Moreover, based on the experimental RC1^e data, a plot of temperature versus time at various stirring rates was devised (Fig. 4). As shown in Fig. 4, the operating conditions did not influence the temperature–time trend. The external conditions did not considerably alter the mass transfer phenomena during the reaction. Therefore, the heterogeneous reaction of CYHPO was attributed to the kinetically controlled reaction regime [19].

Calculation of kinetic parameters of the peroxide reaction

Because of the complexity of the peroxide reaction, CYHPO is always a mixture containing many types of intermediate
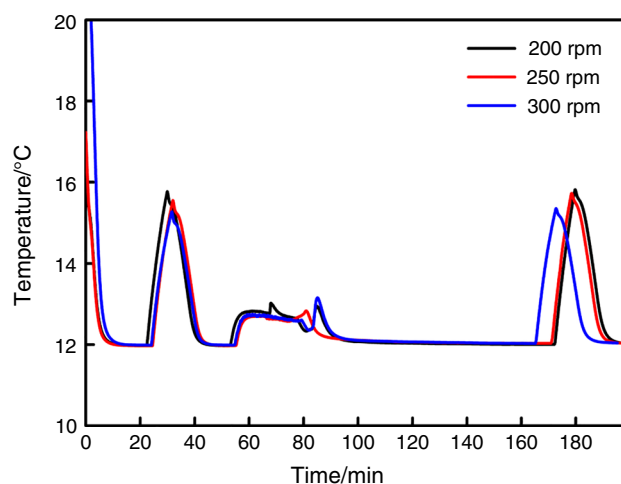

Fig. 4 Reaction temperature as a function of time at various stirring rates

isomers. Obtaining a reaction mechanism of the overall peroxide process by relying solely on experimental data is difficult. Furthermore, from the laboratory to the industrial scale, only scale-up computations must be performed to understand the overall reaction kinetics. In this study, three sets of RC1^e experimental data were fitted using Advanced Kinetics and Technology Solutions–reaction calorimetry simulation software, which is based on mass and heat balance equations [20]. The overall reaction, occurring in the continuous H_2O_2 phase, is as follows (Fig. 5):

The microkinetic equation of the reaction system is defined as

$$2C_6H_{10}O + 2H_2O_2 \rightarrow C_{12}H_{22}O_5 + H_2O \tag{1}$$
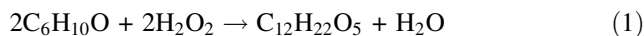
$$r = k_1 C_{C_6H_{10}O}^n C_{H_2O_2}^m \tag{2}$$

This reaction scheme was used as a hypothesis to define various kinetic parameters for the reaction model. Three isothermal RC1^e measurements were performed at 12.0, 15.0, and 18.0 °C. The overall kinetic parameters were determined

Fig. 5 Validation: comparison of the isothermal RC1^e measurement at 15.0 °C with respective simulations by using the optimized reaction kinetic model
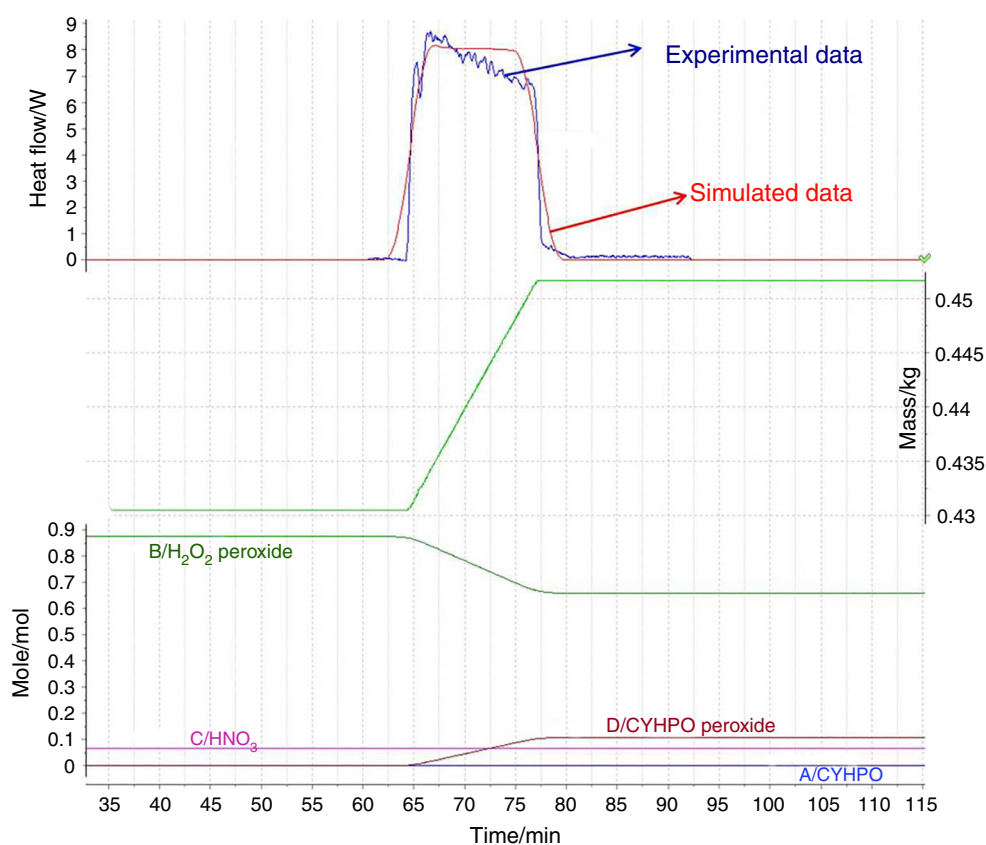

Table 2 Obtained overall kinetic parameters for the CYHPO synthesis

E_α/kJmol^{-1}	Reaction order	A/s^{-1}
110.0	$n = 0.96$	4.21×10^{17}
	$m = 1$	

by performing nonlinear optimization based on the Levenberg–Marquardt algorithm of the obtained calorimetric data (RC1^e) of 12.0 and 18.0 °C, the reaction scheme proposed in Eq. (1), and the reaction rate expression expressed in Eq. (2). The related parameters are listed in Table 2.

To corroborate the optimization reaction model, one simulation was confined to one isothermal RC1^e measurement (Fig. 5). The model fitted the RC1^e measurement adequately. A model is valid only within the range in which it is defined. We performed thermal hazard analysis on the peroxide reaction and a scale-up optimization of this reaction. Consequently, a complete fit of the RC1^e data of a kilogram scale indicated the correct direction for the reaction scheme.

Thermal behavior of products in DSC tests

Figure 6 shows the obtained DSC signals for sample 1 at heating rates of 1.0, 2.0, 4.0, 8.0, and 10.0 °C min^{-1} in a
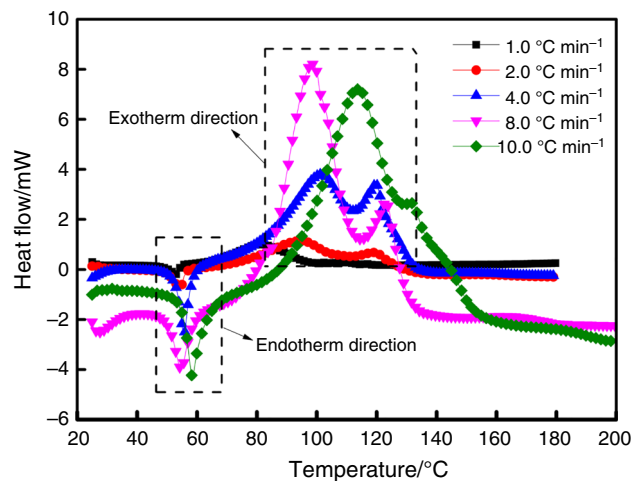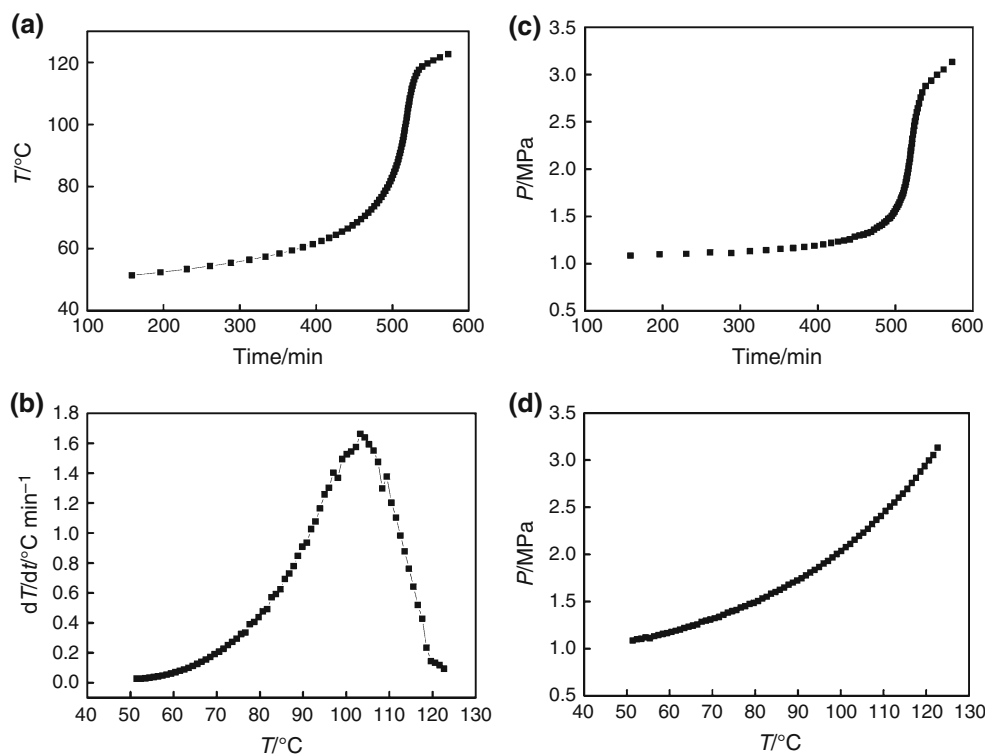

Fig. 6 DSC signals obtained during nonisothermal measurements in dry nitrogen atmosphere at various heating rates

dry nitrogen atmosphere. Table 3 lists the thermal decomposition parameters of sample 1 tested using DSC at various heating rates. The first observed thermal effect in sample 1 was endothermic, and this resulted from melting, which occurred at approximately 50.0–60.0 °C. The incipient of the exothermic reaction of sample 1 was at approximately 90.0–110.0 °C. The initial exothermic

Table 3 Thermal decomposition parameters at various heating rates

	β/°Cmin^{-1}	Mass $\times$ 10^{-1}/ mg	$T_{onset1} \times 10^{-1}$/ °C	$T_{p1} \times 10^{-1}$/°C	$\Delta H_1 \times 10^{-1}$/ J g^{-1}	$T_{onset2} \times 10^{-1}$/ °C	$T_{p2} \times 10^{-1}$/ °C	$\Delta H_2 \times 10^{-1}$/ J g^{-1}
Sample 1	1.0	16.3	500.4	531.9	−461.3	576.6	812.8	5735.7
	2.0	16.7	507.5	543.4	−504.8	743.2	948.7	6868.1
	4.0	16.4	528.5	556.5	−755.8	818.8	1016.7	9642.2
	8.0	16.3	503.4	548.8	−511.6	831.4	983.7	9860.4
	10.0	16.6	550.6	583.7	−531.1	930.9	1137.8	8347.6

Fig. 7 Adiabatic ARC curves of sample 1. **a** A plot of temperature versus time, **b** a plot of self-heating rate versus temperature, **c** a plot of pressure versus time, **d** a plot of pressure versus temperature

temperature of sample 1 was lower than that of pure CYHPO by approximately 10.0 °C at the same heating rate [5]; impurities such as acids favor a secondary reaction. Moreover, a secondary reaction is a frequent occurrence in industrial processes because of the presence of impurities.

Thermal behavior of products in ARC tests

Figure 7 and Table 4 show the thermal behavior of products in the cooling failure scenario. Under adiabatic conditions, the thermal decomposition of CYHPO began at 51.3 °C and ended at 122.0 °C (Fig. 7a). The thermal

hazards associated with the secondary reaction were high. As shown in Fig. 7a, data are scarce at the initial stage because the reaction rate of the unknown thermal decomposition was low, and the experimental default value was 1.0 °C. When the temperature was raised slowly to approximately 60.0 °C, the rate of the temperature rise increased clearly. Figure 7b shows the self-heating rate with the runaway scenario. Afterward, the self-heating rate decreased because of the consumption of reactants, but the temperature of the secondary reaction continued to rise.

Figure 7c and d shows the pressure variations during the exothermic process. The continuous increase in pressure during thermal decomposition suggested that the reaction

Table 4 ARC test on the secondary reaction mixture: thermodynamic properties of reaction mass decomposition

Thermal decomposition parameter	Value
Starting temperature/°C	51.4
Starting pressure/MPa	1.1
Starting self-heating rate/°C min^{-1}	0.027
Final instrumental temperature/°C	122.7
Final instrumental pressure/MPa	3.13
Instrumental adiabatic temperature rise/°C	71.3
Thermal inertia factor/dimensionless	4.7
Adiabatic temperature/°C	337.0
Final reaction temperature/°C	388.5
Maximum temperature rise rate/°C min^{-1}	1.64
Decomposition enthalpy/J g^{-1}	288.1
Time to maximum rate under adiabatic conditions/min	260.7

Fig. 8 Experimental and simulated curves of decomposition under adiabatic conditions

generated several gaseous products. In ARC measurements, heat generated by the thermal decomposition of a sample was applied on the titanium alloy bomb; therefore, the consideration of the thermal inertia factor was necessary [1, 18], which was not defined in this study. The thermal decomposition parameters listed as commencing at 1.64 °C min^{-1} in Table 4 were already corrected by thermal inertia.
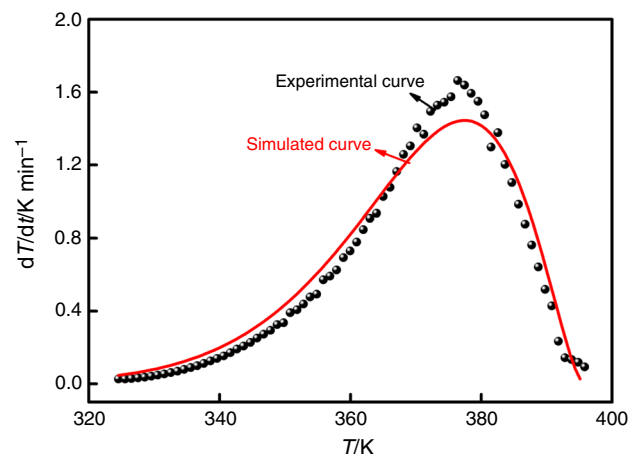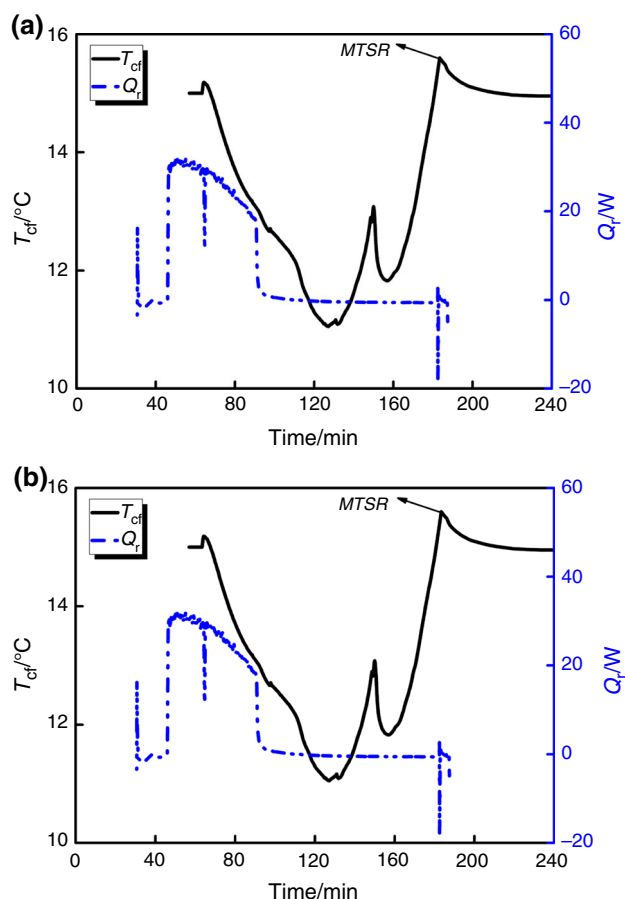
Adiabatic kinetic parameters

Equation 3 was used to obtain the thermal decomposition kinetic parameters determined by performing the adiabatic test [18]. According to Eq. (3), by selecting an appropriate reaction order n, a plot of $\ln(m_T / \Delta T((T_f - T)/\Delta T)^n)$ versus $1/T$ rendered a straight line, where the values of apparent activation energy (E_a) and frequency factor (A) were acquired from the slope and intercept, respectively.

$$\ln\left(\frac{m_T}{\Delta T((T_f - T)/\Delta T)^n}\right) = \ln A - \frac{E_a}{RT} \quad (3)$$

where m_T is the self-heating rate at an arbitrary temperature, T_f is the measured final temperature, ΔT is the measured adiabatic temperature increase, T is the absolute temperature, n is the reaction order, and R is the universal gas constant.

According to Eq. (3) and based on the nonlinear fitting method, when $n = 1.7$, the linear correlation coefficient (0.972) was the highest, and E_a and A were 112.0 kJ mol^{-1} and 1.9×10^{15} mol$^{-0.7}$ L$^{0.7}$s^{-1}, respectively. Figure 8 shows the adiabatic kinetic fitting curve. As shown in Fig. 9, the experimental curve was a close fit with the

Fig. 9 MTSR and T_{cf} curves of the desired reaction at 12.0 °C and 250 rpm. **a** Two curves without correction, **b** *MTSR* curve corrected by the yield

simulation curve. In addition, the time to maximum rate under adiabatic decomposition conditions (*TMR*$_{ad}$) can be determined using E_a, A, and n [18]. The temperature at

Table 5 Thermal hazard parameters of the peroxide reaction

Test no.	Reaction temperature/°C	Stirring rate/rpm	M_{cy}/g	Dosing time/min	ΔT_{ad}^a/°C	ΔT_{ad}^b/°C	$MTSR^a$/°C	$MTSR^b$/°C
1	12.0	250.0	166.0	120.0	40.6	43.1	15.6	16.6
2	15.0	250.0	166.0	120.0	41.2	44	16.7	17.8
3	18.0	250.0	166.0	120.0	44.0	46.2	17.3	18.2
4	12.0	200.0	166.0	120.0	40.2	43.6	16.5	17.6
5	12.0	250.0	166.0	115.0	45.2	47.7	15.2	16.1
6	12.0	300.0	166.0	120.0	47.3	50.3	14.7	15.6
7	12.0	250.0	150.0	113.0	40.1	42.4	15.2	16.1
8	12.0	250.0	166.0	125.0	39.8	42.2	13.8	14.5
9	12.0	250.0	210.0	158.0	50.2	54.2	16.1	17.4

[a] Data from test

[b] Data corrected by yield

which $TMR = 24$ h (T_{D24}) of sample 1 was evaluated to be approximately 15.8 °C.

Thermal hazard evaluation

The heat generated from a secondary reaction is typically higher than that from the desired reaction. Any safer chemical process should avoid or manage undesirable decomposition. The optimized reaction process can be identified by employing the maximum temperature of the synthesis reaction (MTSR) of the desired reaction (Eq. 4) and T_{D24} of the secondary decomposition [13, 14].

$$MTSR^a = T_p + \frac{\max(Q_{accu})}{C_p M_r} = T_p + \frac{\max(Q_{input} - Q_{exo})}{C_p M_r}$$
$$= T_p + \frac{\max\left(\frac{\Delta Hm_{cy}}{M_{cy}} - Q_{exo}\right)}{C_p M_r} \qquad (4)$$

where T_p is the reaction temperature, Q_{accu} is the accumulated energy, Q_{input} is the potential input energy, Q_{exo} is the measured heat generation, C_p is the specific heat capacity of the co-reactant, M_r is the reactant mass in the reactor, ΔH is the measured overall heat of the reaction, m_{cy} is the cyclohexanone mass that has been charged into the reaction during a given time, and M_{cy} is the overall cyclohexanone mass charged into the reactor.

According to the RC1^e measurement results, <10 % of initial cyclohexanone was contained within the reactor after the experiments. Although cyclohexanone reacted with H_2O_2, only if the reactant was heated or the reaction conditions were changed abruptly would the remaining reactant have reacted again. Therefore, the reaction heat and MTSR (Eq. 5) should be modified for thermal loss prevention as follows:

Table 6 Temperatures to determine the criticality classes of various conditions for the peroxide reaction

Test no.	T_p/°C	M_{cy}/g	MTSR/ °C	MTT/ °C	T_{D24}/°C	Class
1	12.0	166.0	16.6	120.0	15.8	V
2	15.0	166.0	17.8			V
3	18.0	166.0	18.2			V
8	12.0	150.0	14.5			II
9	12.0	210.0	17.4			V

$$MTSR^b = T_p + \frac{\max\left(\frac{\Delta Hm_{cy}}{YM_{cy}} - Q_{exo}\right)}{C_p M_r} \qquad (5)$$

where Y is the yield of the peroxide reaction.

The adiabatic temperature rise ΔT_{ad}, denoted in Eqs. (6) and (7), was also determined, and ΔT_{ad}^a and ΔT_{ad}^b were calculated as follows:

$$\Delta T_{ad}^a = \frac{\Delta H}{C_p M_r} \qquad (6)$$

$$\Delta T_{ad}^b = \frac{\Delta H}{C_p M_r Y} \qquad (7)$$

$$T_{cf} = T_p + \Delta T_{ad} \qquad (8)$$

where T_{cf} is the maximum adiabatic temperature rise caused by thermal accumulation at a given time. Therefore, MTSR can be defined as follows:

$$MTSR = \max(T_{cf}) \qquad (9)$$

Figure 8 shows the MTSR and T_{cf} curves under the reaction conditions of 12.0 °C and 250 RPM, respectively, in accordance with Eqs. (8) and (9). Other MTSRs of various reaction conditions are listed in Table 5.

Based on the thermal runaway scenario, the criticality class of this process under various reaction conditions was calculated (Table 6) [13, 14]. The *MTSR* is listed in Table 5. The reaction was conducted in an open system, and the mass of the concentrated HNO_3 catalyst was left unchanged; therefore, for technical reasons, the maximum temperature was the normal boiling point of concentrated HNO_3, 120 °C.

As listed in Table 6, except for Test 8, the criticality classes for the other tests were five. Although the reaction temperature of the peroxide process is lower than 20 °C at the industrial scale, once the chemical process undergoes cooling failure or if stirring is stopped abruptly, the system enters adiabatic conditions, which may lead to critical chemical accidents. A criticality class of five is theoretically insupportable. The risks can be reduced if the process itself is altered to avoid the triggering of a secondary reaction. Based on the results of Test 8, if the productivity is admissible, a reduction in the mass of cyclohexanone can alleviate the risk of the thermal runaway scenario in a semi-batch reactor.

Conclusions

The thermal hazards of CYHPO synthesis and the criticality classes were investigated using RC1^e, DSC, and ARC. The results revealed that the adiabatic temperature of the peroxide reaction may increase to 50 °C, which is extremely hazardous. According to the RC1^e measurements, a heterogeneous liquid–liquid peroxide reaction belongs to the kinetically controlled reaction regime. The overall reaction kinetic parameter was simulated (simulation curve), and it was a close fit with the experimental curve. DSC and ARC experiments indicated that NHO_3 and impurities may catalyze the decomposition of CYHPO, thereby increasing the thermal hazards associated with a secondary reaction. According to the *MTSR* of the desired reaction and T_{D24} of secondary decomposition, except for the decreasing mass of cyclohexanone, the criticality classes of other conditions were five, which were unacceptable. Therefore, the results can be used for establishing safe conditions for exothermal processes on a commercial scale.

References

1. Yang D, Koseki H, Hasegawa K. Predicting the self-accelerating decomposition temperature (*SADT*) of organic peroxides based on non-isothermal decomposition behavior. J Loss Prev Process Ind. 2009;16(5):411–6.
2. Malow M, Wehrstedt KD. Prediction of the self-accelerating decomposition temperature (*SADT*) for liquid organic peroxides from differential scanning calorimetry (DSC) measurements. J Hazard Mater. 2005;A120:21–4.
3. Boseh CM, Velo E, Recasens E. Safe storage temperature of peroxide initiators: prediction of self-accelerated decomposition temperature based on a runaway heuristics. ChemEng Sci. 2001;56(4):1451–7.
4. Chou HC, Chen NC, Hsu ST, Wang CH. Runaway reaction and thermal hazards simulation of cumenehydroperoxide by DSC. J Loss Prev Process Ind. 2008;21(1):101–9.
5. Zang N, Qian XM, Huang P, Shu CM. Thermal hazard analysis of cyclohexanone peroxide and its solutions. Thermochim Acta. 2013;568:175–84.
6. Zang N, Qian XM, Liao JY, Shu CM. Thermal stability of lauroyl peroxide by isoconversional kinetics evaluation and finite element analysis. J Taiwan Inst Technol. 2014;45(2):461–7.
7. Sebastien L, Lionel E, Cyril C. Thermal risk assessment of vegetable oil epoxidation. J Therm Anal Calorim. 2015;122:795–804.
8. Lee MH, Chen JR, Das M, Hsieh TF, Shu CM. Thermokinetic parameter evaluation by DSC and TAM III along with accountability of mass loss by TG from the thermal decomposition analyses of benzoyl peroxide. J Therm Anal Calorim. doi:10.1007/S10973-015-4917-1.
9. Chen WT, Chen WC, You ML, Tsai YT, Shu CM. Evaluation of thermal decomposition phenomenon for 1,1-bis(*tert*-butylperoxy)-3,3,5-trimethylcyclohexane by DSC and VSP2. J Therm Anal Calorim. doi:10.1007/s10973-015-4985-2.
10. Lin SY, Shu, CM, Tsai YT, Chen WC, Hsueh KH. Thermal decomposition on Aceox BTBPC mixed with hydrochloric acid. J Therm Anal Calorim. doi:10.1007/s10973-015-4895-3.
11. Chen LP, Liu TT, Yang Q, Chen WH. Thermal hazard evaluation for iso-octanol nitration with mixed acid. J Loss Prev Process Ind. 2012;25(3):631–5.
12. Gygax R. Chemical reaction engineering for safety. ChemEng Sci. 1988;43(8):1759–71.
13. Gygax R. Scale up principles for assessing thermal runaway risks. ChemEng Sci. 1990;43(8):53–60.
14. Stoessel F. Thermal safety of chemical processes-Risk assessment and process design. Weinheim: Wiley; 2008.
15. Zeng XL, Chen WH, Wang FW. Experimental study on thermal stability of EHN. China Saf Sci J. 2009;19(8):67–72.
16. Code for first batch of hazardous chemical processes on the key directory regulators. Beijing: State Administration of Work Safety, 2009.
17. Code for second batch of hazardous chemical processes on the key directory regulators. Beijing: State Administration of Work Safety, 2013.
18. Townsend DI, Tou JC. Thermal hazard evaluation by an accelerating rate calorimeter. Thermochim Acta. 1980;37:1–30.
19. Francesco M, Renato R. Thermally safe operation of liquid-liquid semi-batch reactors. Part I: single kinetically controlled reactions with arbitrary reaction order. ChemEng Sci. 2005;60(12):3309–22.
20. AKTS-Thermokinetics Reaction Calorimetry Software, AKTS, AG, Advanced kinetics and technology solutions. 2015. http://www.akts.com.